Full Paper

DESIGN OF AERODYNAMIC PARTS TO REDUCE DRAG COEFFICIENT OF A PASSENGER VAN

Vasaphon Sinsab* Dulyachot Cholaseuk

Department of Mechanical Engineering, Thammasat School of Engineering, Thammasat University, 99, Moo 18, Phaholyothin Rd., 12120, Klongluang, Pathumthani, Thailand

Graphical abstract

(a)

(b)
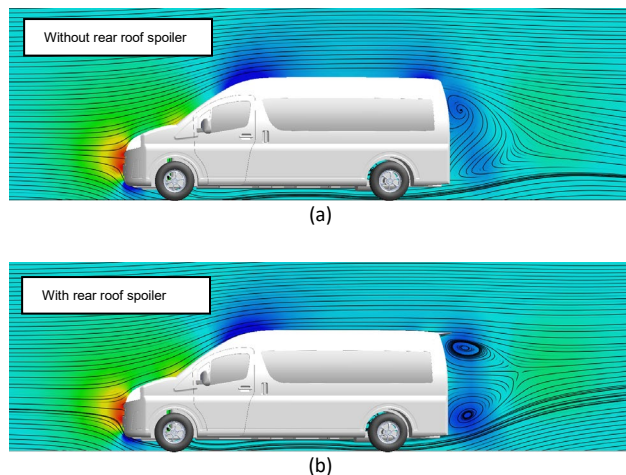
Abstract

Air resistance plays a significant role in vehicle energy consumption. Commercial passenger vans with 7 - 12 seats are widely used for public transportation across Thailand. Most passenger vans were designed in near-rectangular shapes to maximize cabin space, which is considered poor aerodynamic efficiency and results in high fuel consumption at cruising speed. This research focused on finding suitable aerodynamic parts to reduce air resistance on such vans. The most popular van model was used as a basis for the study. It has a drag coefficient of 0.36. Effects of various aerodynamic parts on the drag coefficient reduction were studied computationally at 90 kilometers per hour wind velocity using SolidWorks Flow Simulation software. The results showed that a rear roof spoiler is the most effective aerodynamic part. Upon optimizing the spoiler geometry, the drag coefficient is reduced to 0.32. This resulted in an 5.63% reduction in fuel consumption.

Keywords: Van's Aerodynamic, Aerodynamic parts, Reduce Drag Coefficient, Computation Fluid Dynamic, Aerodynamics properties of van's fuel economy.

1.0 INTRODUCTION

In Thailand, passenger vans are one of the most popular forms of transportation, including personal vans, agency vans, delivery vans, emergency vans, and the most popular commercial passenger vans. According to the 2022 Transport Statistics Report, the Department of Land Transport has registered a total of 445,862 seven seated or more passenger cars, comprising 33,188 air-conditioned vans [1], 8,859 regular-routed, 22,787 non-regular-routed, and 1,542 privates [2].

Most commercial passenger vans are much less aerodynamically efficient than sedans and SUVs. A large commercial vehicle, such as a big truck, loses about 52% of the total fuel consumption in overcoming air resistance along generally 130,000 - 160,000 km of working distance per year.[3]

Most vans do not install aerodynamic parts to reduce air resistance. Furthermore, some install additional parts but only for aesthetic purposes. Only racing, sports, and authentic premium cars look for the numerical values in engineering, energy, and the environment for the best performance.

Designs to improve the drag coefficient of vehicles have been constantly evolving since the early 20th century for better speed, fuel consumption, engine efficiency, and driving performance. Most antique cars did not consider aerodynamic properties, giving them most an angular shape. Over time, more research on fluid dynamics and aerodynamics has been established, beginning with the primary form of study, such as the design of minimum drag bodies in incompressible laminar flow [4] of finding a two-dimensional shape with minimal air resistance, which mentions both drag force and skin friction, then the aerodynamic research of a racing car based on wind

tunnel test and computational fluid dynamics [5]. As a result, modern vehicles have a better aerodynamic body shape.

Drag refers to the force exerted by a flowing fluid on an object in the direction of flow. It consists of normal pressure forces and tangential shear forces due to viscous effects. Both forces have components in the direction of flow, resulting in the drag force being the combined effect of pressure and wall shear forces (skin friction force) in that direction.

On the other hand, the lift is the sum of the components of pressure and wall shear forces in the direction normal to flow, which tend to move the object in that direction.

Dimensionless numbers representing the object's drag and lift characteristics are commonly used for convenience. These numbers are the drag coefficient C_D and the lift coefficient C_l.

There are various inventions for improving the aerodynamic efficiency of vehicles. For example, Gatto et al. patented the US-2022410985-A1 [6], showing that the components installed in the container's rear can reduce C_D to 9.7%. Moradnia et al. patented US-20230013812-A1 [7], a device designed for mounting on a vehicle's four-wheel structure to improve the brakes' cooling properties and aerodynamics around the wheels. Rose et al. patented US-20220402564-A1 [8]. It is a development and design of a spoiler that can be retracted depending on the speed of the car's movement, improving its drag efficiency, which is suitable for various driving situations.

Various researchers attempted to find novel approaches to reduce the aerodynamic drag of different types of vehicles, such as research by Laipradit et al. (2000) [9]. Their studies conclude that closing the pickup area will reduce C_D by 29.41% because the truck's airflow is smoother, and reducing frontal air pressure by a 15 cm wedge frontal dam installed as a bus skirt can reduce C_D by 7%. Hariram et al. (2019) [10] explored more than fifteen aerodynamic parts, resulting in about 25% less energy consumption of a heavy-duty vehicle by combining multiple attached parts to area's problems such as trimming the shape edge of the trailer, covering the space under the car between the towing vehicle and the trailer, and deflecting airflow off the sharp cabin. However, no official or reliable open research data regarding aerodynamic devices' effects on improving van aerodynamic properties for fuel economy. Therefore, this research aims to provide information for public use in Thailand and other countries interested in using it to promote energy conservation policies. This is considered an option for energy conservation that has enormous positive impacts, such as promoting the production of automotive parts that are beneficial to drivers, the environment, and the economy.

This paper analyzed vans at a constant average speed of 90 kilometers per hour, a speed limit for driving on the road according to Thailand's transportation law [11]. The airflow behaviors passing the van were studied through the CFD (Computational Fluid Dynamics) method with SolidWorks Flow Simulation software [12] based on the principle of Navier–Stokes equations [13] to identify the problem areas that caused air resistance and then improve the airflow characteristics in these areas, leading to the design of the aerodynamic parts that can reduce the drag coefficient.

2.0 MODELING AND SIMULATION

This section details modeling, setup, and flow simulations in SolidWorks. The magnitude of drag and lift forces obtained from the simulations will be used to compute the drag coefficient C_D and the lift coefficient C_L from the following equations.

Drag coefficient:

$$C_D = F_D / 0.5\rho V^2 A \qquad (1)$$

Lift coefficient:

$$C_L = F_L / 0.5\rho V^2 A \qquad (2)$$

F_D is the drag force, F_L is the lift force, ρ is the density of the fluid, V is the upstream velocity, and A is the object's frontal area.

2.1 Dimension of a Van

The most popular van used for public transport in Thailand is selected to be a 3D model prototype to study flow patterns and air properties as it flows past the body—the prototype dimension, as shown in Figure 1 and detail in Table 1
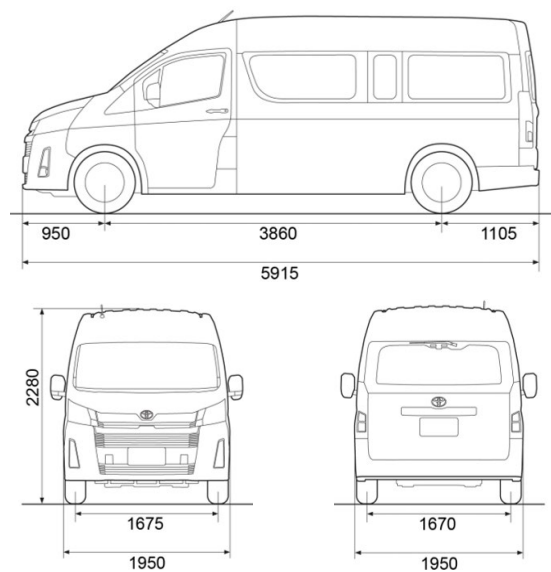

Figure 1 2D Van Dimension is described in millimeter units [14].

Table 1 Specifications of the model

No.	Parameters	Dimension Values
1	Width (m)	1.95
2	Length (m)	5.915
3	Height (m)	2.28
4	Front wheelbase (m)	1.675
5	Rear wheelbase (m)	1.67
6	Wheelbase (m)	3.86
7	Tire	235/65R16C
8	Gross weight (kg)	3,820
9	Frontal area (m²)	3.957

2.2 Computational Domain

The Computational Domain defines the size of the simulated wind tunnel. The size must be appropriate because it will affect the air pressure results and other features. It excessively consumes computer resources and takes longer to simulate than necessary if it is too large. By trial to correct size several times. The optimal computational domain size has been accomplished, as shown in Figure 2.
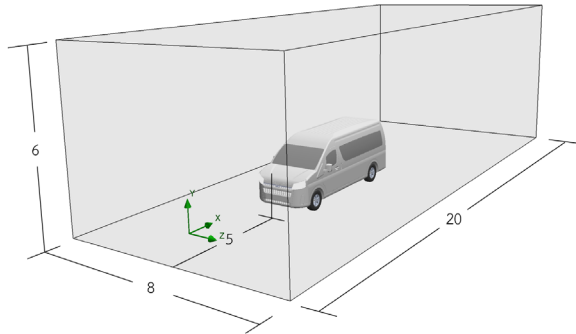
Figure 2: Computational domain in meter units.

2.3 Simulation

The flow simulation model, air properties, and boundary conditions are specified in Table 2.

Table 2 Simulation settings.

Conditions	Parameters	Values
Analysis type	External	
Physical Features	Fluid Flow	
Project Fluids	Air (Gases)	
Turbulence	Turbulence intensity	0.1%
	Turbulence length	0.02264 m
Governing Equation	Navier-Stokes Equation, k–ε turbulence model, FANS [12]	
Default wall thermal condition	Adiabatic wall	
Roughness	0 micrometer	
Thermodynamic Parameters	Pressure	101,325 Pa
	Temperature	293.2 K
Velocity Parameters	Defined by	3D Vector
	Velocity in X direction	25 m/s
	Velocity in Y direction	0 m/s
	Velocity in Z direction	0 m/s

2.4 Meshing

SolidWorks Flow Simulation has three meshing selections, each of which can be refined in many ways. This adjustment affects the accuracy of the simulation results, convergence iterations, and duration time. Therefore, all three systems have been explored many times at different levels of refinement. It can be concluded that the mesh system that gives the most accurate results is the Global Manual Mesh at maximum refinement of level 6. The results of the meshing 3D model van without aerodynamic parts consist of 3,995,121 cells, dividing 3,995,121 fluid cells as 2,043,401 contacting cells (as shown in Figure 3).
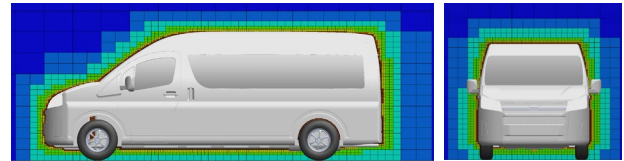

Figure 3 Meshing grid

2.5 Flow Simulation Result

The results of the airflow simulation over the van without aerodynamic parts are shown in Figures 4 to 6. Upon analyzing the force acting on the vehicle, a drag coefficient of 0.362 is obtained. Details are shown in Table 3

Table 3 Drag force obtained from the simulation.

Numerical results	Values
Pressure Drag (N)	514.882
Skin Friction Drag (N)	23.732
Lift Force (N)	371.527
Drag Coefficient: C_D	0.362
Reynold's number	$\approx 3.7 * 10^6$

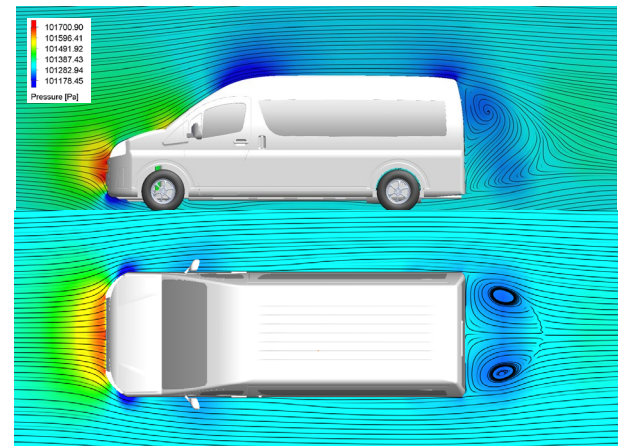Thus, Drag Force (F_D) [15] is equal to 538.614 N

Figure 4: Pressure distribution and streamlines.

According to the pressure contour in Figure 4, high pressure at the nose of the vehicle contributes to a significant part of pressure drag. In contrast, the transition from the front hood to the windshield also plays an important role. The low-pressure area from air swirls behind the vehicle also increases pressure drag.

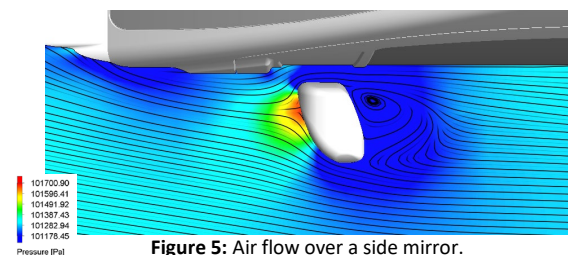Stagnation pressure over the massive side mirrors also adds more pressure drag to the vehicle (as shown in Figure 5).
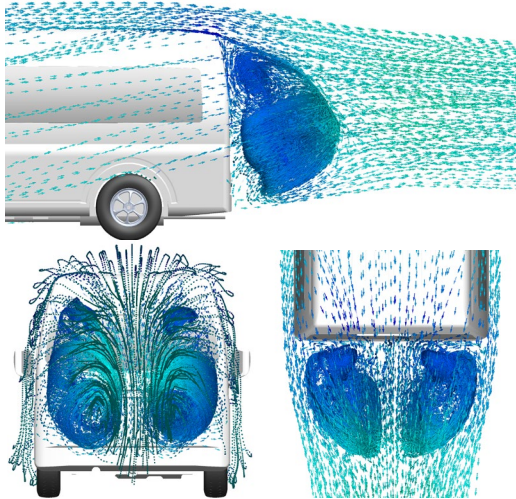

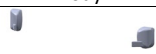**Figure 5:** Air flow over a side mirror.

Figure 6: Rear air swirls.

Figure 6. shows the direction of air mass behavior at the model's rear. It is an area where large air swirls occur caused by the air flowing over the roof's curved surface, forced to move faster than the air passing the sides and under the model, especially at the leading-edge door boot, thus creating lift force.

2.6 Proportion of Drag Force Generated by The Van

The hypothesis that removing the large side mirrors of the van will help reduce drag force is correct. Removing both side mirrors reduces air resistance by 9.48 N (1.76%). However, this option was not considered in this research because the alternative rear-view camera system is still impractical (Table 4).

Table 4 Shows the proportion of drag force to the van.

Main Van's Portions	Drag Force (N)	Frontal Area (m^2)
Body	527.088 (97.86%)	3.733 (94.34%)
Side mirrors	9.48 (1.76%)	0.1025 (2.59%)
Wheels	2.046 (0.38%)	0.121 (3.07%)

The frontal area and total drag force are mentioned in Table 1. and Table 3. respectively.

3.0 DESIGN OF AERODYNAMIC PARTS

The airflow pattern and pressure distribution from the simulation in section 2.5 provide insight into positions that could be aerodynamically improved. Section 3.0 explores the effects of installing aerodynamic parts on those positions.

3.1 Study of Effects of Various Aerodynamic Parts on C$_D$

Five positions were targeted where the airflow could be modified to reduce drag (Figure 7).

1. The front grille
2. The front wheels run directly against the wind.
3. Connecting the bonnet to the windshield
4. Side mirrors
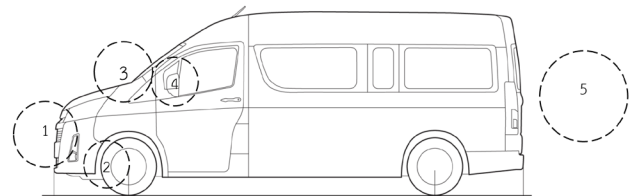5. The swirling wind at the rear of the model.

Figure 7 Targeted positions.

Different aerodynamic parts were applied to the five positions, as shown in Figure 8.

a. Front Skirt   b. Front Wheel Air Deflector

c. Windshield Air Deflector   d. Side Mirror Nose
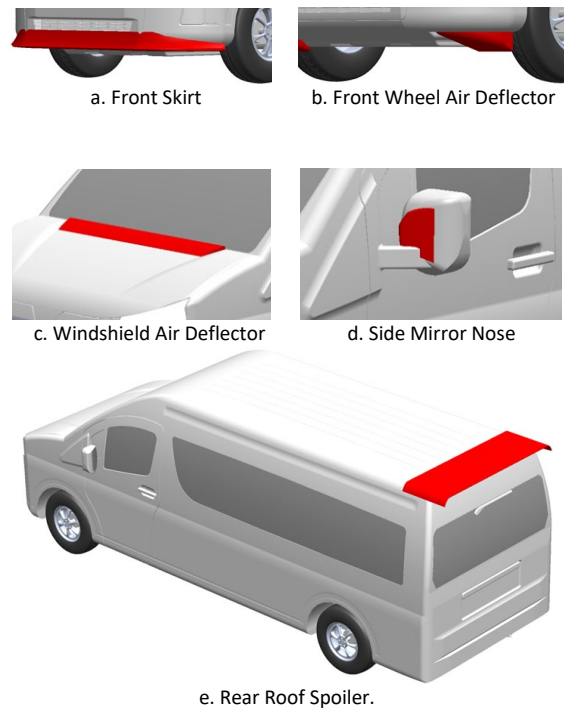

e. Rear Roof Spoiler.

Figure 8 Five initial designs of aerodynamic parts.

Flow simulation results in Table 5 consist of the van's drag force, lift force, and drag coefficient with different aerodynamic parts installed.

Table 5 Drag and lift on the van after installing the parts.

| Parts	Drag Force (N)	Lift Force (N)	C_D
a	697.397	428.259	0.469
	(+ 29.48 %)	(+15.27 %)	(+ 29.48 %)
b	534.574	388.84	0.359
	(- 0.75 %)	(+4.66 %)	(- 0.75 %)
c	537.106	369.892	0.361
	(- 0.28 %)	(-0.44 %)	(- 0.28 %)
d	539.045	371.527	0.362
	(+ 0.08%)	(0 %)	(+ 0.08%)
e	500.049	184.129	0.336
	(- 7.16%)	(-50.44 %)	(- 7.16%)

% results in comparison to values without aerodynamic part.
(- %) desirable. (+ %) undesirable.

Table 4 shows that the installation of part e, the rear roof spoiler, reduced the drag coefficient by 7.16%, which is the most significant reduction. Hence, the rear roof spoiler is the most critical aerodynamic part that should be installed on the van. The geometry of the spoiler is then optimized for more drag reduction.

3.2 Optimization of Rear Roof Spoiler Geometry

The basic geometry of the rear roof spoiler is defined by three parameters: length, tilt angles, and taper angle, as shown in Figure 9. Utilizing a uni-direction search scheme, each parameter was optimized sequentially.
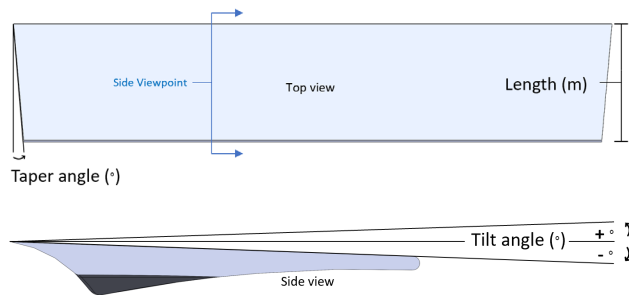
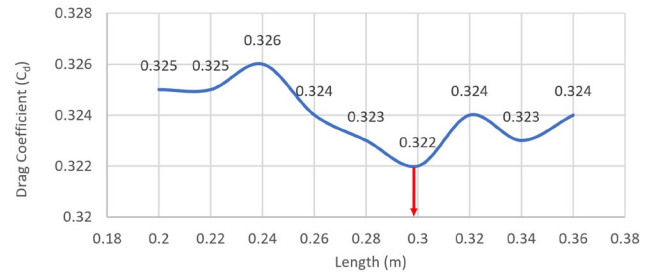**Figure 9** Design parameters of the rear roof spoiler.

3.2.1 Length

The length is the optimal x-axis length when simulated under Global Manual Mesh, with refinement level 6 giving the lowest drag coefficient.

Table 6 Searching for optimum spoiler length

Length (m)	C_D	Lift Force (N)	Drag Force (N)
0.20	0.325	227.354	484.128
0.22	0.325	225.648	484.057
0.24	0.326	242.032	485.506
0.26	0.324	228.639	482.929
0.28	0.323	235.303	480.810
0.30	0.322	239.403	480.135
0.32	0.324	229.818	482.512
0.34	0.323	237.093	481.168
0.36	0.324	231.655	481.824

Table 6 shows the division of the length into 0.02 m intervals. At a length of 0.3 m, it gives the lowest 0.322 drag coefficient, which decreased by 11.05% (as shown in Figure 10).
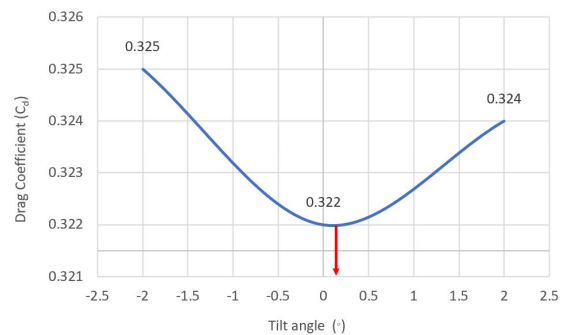

Figure 10 Lowest C_D at 0.3 m Length.

3.2.2 Tilt angle

The tilt angle is the optimal x-axis angle when simulated under Global Manual Mesh, with refinement level 6 giving the lowest drag coefficient.

Table 7 Searching for the optimum tilt angle.

Length (m)	Tilt Angle (°)	C_D	Lift Force (N)	Drag Force (N)
0.3	+2	0.325	212.384	483.565
0.3	0	0.322	239.403	480.135
0.3	-2	0.324	258.907	481.696

Table 7 shows the division of the tilt angle into small intervals of 2 degrees. Any minor adjustment in the tilt angle can increase the drag coefficient, so additional randomization is deemed unnecessary. The simulation shows that at a tilt angle of 0 degrees, it gives the lowest 0.322 drag coefficient, which decreases by 11.05% (as shown in Figure 11).
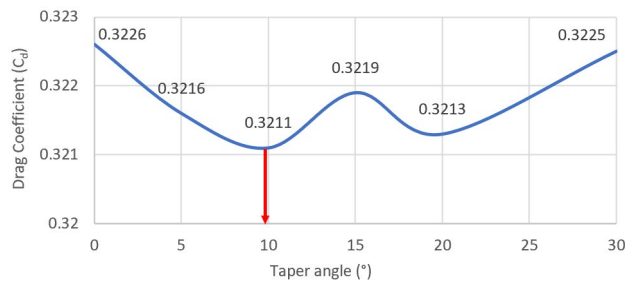

Figure 11 Lowest C_D at 0 ° tilt angle.

3.2.3 Taper angle

The taper angle is the cutting angle from the top view of the spoiler when simulated under Global Manual Mesh, with refinement level 6 giving the lowest drag coefficient.

Table 8 Searching for the optimum taper angle.

Length (m)	Tilt Angle (°)	Taper Angle (°)	C_D	Lift Force (N)	Drag Force (N)
0.3	0	0	0.323	240.209	480.202
0.3	0	5	0.322	237.269	478.717
0.3	0	10	0.321	235.657	477.976
0.3	0	15	0.322	235.07	479.224
0.3	0	20	0.321	236.153	478.258
0.3	0	30	0.323	235.716	480.086

Table 8 shows the division of the taper angle into 5-degree intervals. Increasing the taper angle can decrease the drag coefficient and gradually increase it after passing the optimum point. At a taper angle of 10 degrees, give the lowest 0.321 drag coefficient, which decreases drag by 11.33%. From the increasing and decreasing behavior of the drag coefficient, it can be concluded that the lowest value only exists at a particular point. The drag coefficient increases gradually when increasing/decreasing the taper angle beyond this point. Illustrate in Figure 12.

**Figure 12:** Lowest C_D at 10 ° taper Angle.

From the results of the uni-direction search, the optimum parameters of the rear roof spoiler are 0.3-meter length, 0-degree tilt angle and 10-degree taper angle. Figure 13 shows the rear roof spoiler with the optimum parameters.
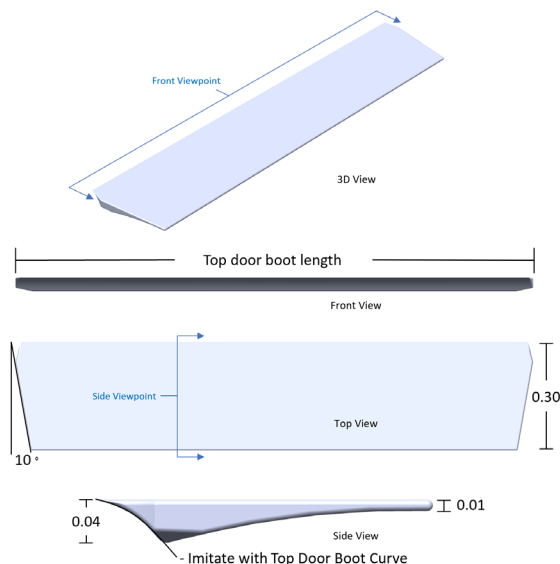
Figure 13: Rear roof spoiler with optimum parameters.

3.4 Exploring Additional Features for Rear Roof Spoiler

The effect of additional features is explored to seek a further reduction in the drag coefficient. Inspired by observations not only of nature, such as birds and marine animals, but also technology from other industries to try and adapt, e.g., the pressure holes, the dimple of a golf ball surface, and Siddiqui et al. aircraft wings tips [16], to study and simulate how these unique features affect spoiler.

Thirteen additional features have been applied to the rear roof spoiler to explore the possibility of further drag reduction.
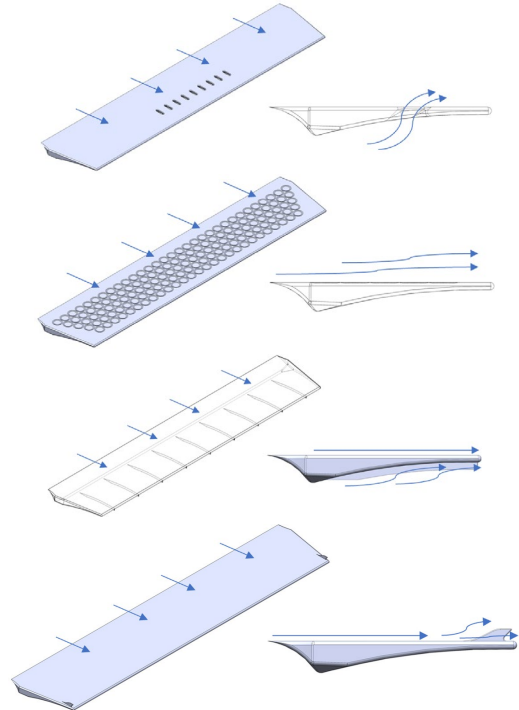
Figure 14: Example from thirteen additional features.

Table 9 Thirteen features and drag coefficient results.

Model No.	Drag Coefficient	Features
Model 0	0.3202	l design
Model 1	0.324	1-Row rectangular hole
Model 2	0.321	1-Row middle oval hole
Model 3	0.324	1-Line smooth cut
Model 4	0.323	Sharkskin [17]
Model 5	0.321	Big golf dimple pattern
Model 6	0.323	Small golf dimple pattern
Model 7	0.322	Air fin
Model 8	0.322	Small upper side fin
Model 9	0.321	Big upper side fin
Model 10	0.321	Big under side fin
Model 11	0.322	10 degrees front cut
Model 12	0.3203	Smooth tangent top view cut
Model 13	0.32	Front view curve cut (Falcon side profile)

Simulation results with various additional features integrated with the spoiler's profile show that multiple types of holes hope to take advantage of the difference in air pressure between the

upper and the lower part of the spoiler for higher air pressure under the spoiler, which is turbulence can automatically run up through the holes vented to the air above thus reduce the amount of air turbulence. Still, the results showed that those holes made natural airflow more complex, increasing the drag coefficient. Shark skin and fins were ineffective as they increased the frontal area. The golf dimple pattern also cannot give positive results since the spoiler does not have a symmetrical dimple pattern. Thus, it does not meet the hypothesis of aerodynamics of a golf ball with grooves [18], detailing that golf balls have less drag coefficient than smooth spheres. The best feature here is the front curve cut in Model 13, considered the optimum rear roof spoiler (details are shown in Table 9as well as Figures 15 and 16).
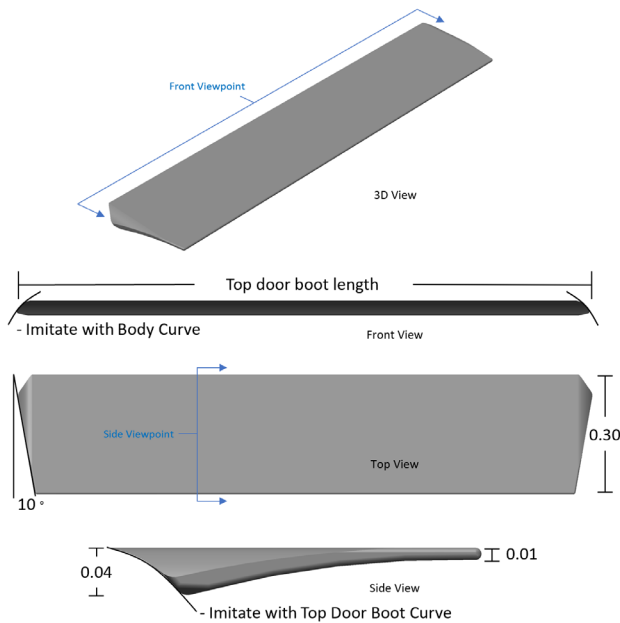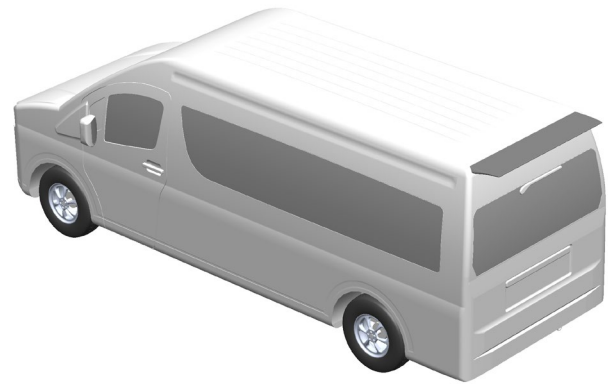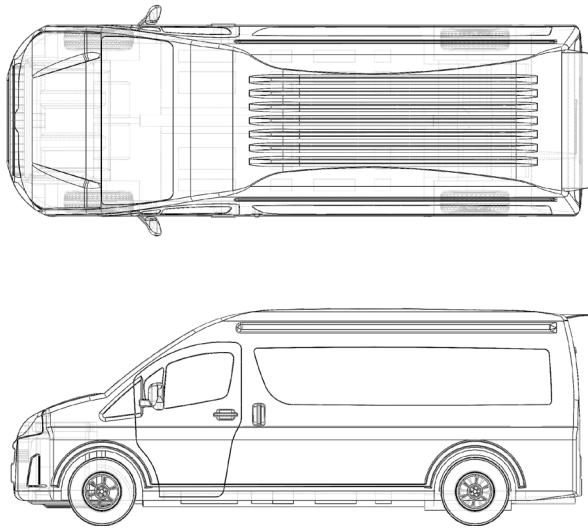

Figure 15: Optimum rear roof spoiler.

Figure 16: 3D Van with an optimum rear roof spoiler.

4.0 RESULTS AND DISCUSSION

The optimum rear roof spoiler installation resulted in an 11.6% drag reduction, as detailed in Table10.

Table 10 Results of the Optimum Rear Roof Spoiler.

Data results	Van 3D Model	With Model 13	% Change
Drag Coefficient	0.362	0.32	- 11.6 %
Drag Force (N)	538.614	475.967	- 11.6 %
Lift Force (N)	371.527	234.783	- 36.8 %

* The spoiler's skin friction is sorely insignificant.

(- %) desirable. (+ %) undesirable.

4.1 How the Rear Roof Spoiler Reduces Van's Drag and Lift

In Figure 17. The pressure contour difference clearly shows that when the spoiler is installed, the air pressure and streamline change positively. The air pressure at the leading-edge door boot and the trailing area increases, and although air swirls remain relatively more prominent, the magnitude changes from large to smaller ones. Figure 18. shows the difference in flow trajectories. There are two high-density large air swirls in the model without the spoiler. In the model with the spoiler, the air swirls occur with a much smaller density. These result in significantly reduced drag and lift force.
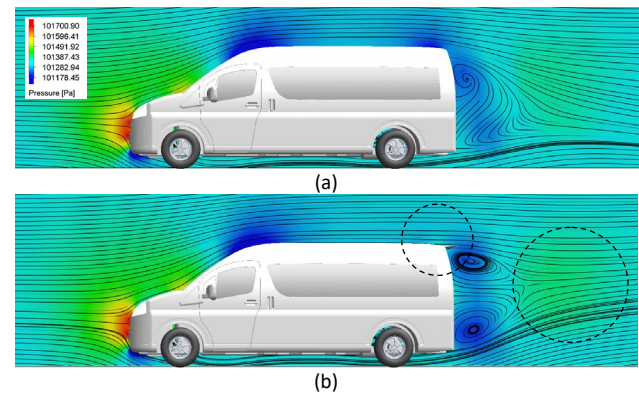

Figure 17 Comparison of streamlining and pressure distribution around the van (a) without and (b) with a rear roof spoiler.
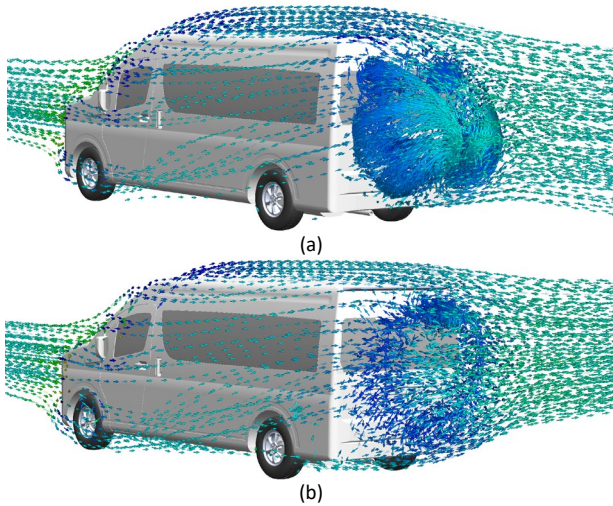
Figure 18 Comparison of air swirls rearward of the van (a) without and (b) with a rear roof spoiler.

4.2 Performance, Economic and Environmental Impact

Making assumptions and simulation principles to reduce front wind buffeting and air swirls at the vehicle's rear, installing an optimum rear roof spoiler (Model 13) minimizes the van's drag coefficient from 0.362 to 0.32 (11.6% reduction). The spoiler could significantly reduce fuel consumption at cruising speed and CO_2 emissions and represent a 36.7% reduction of lift force, resulting in improved stability and brake efficiency in various driving scenarios.

For better understanding, simple calculations for a public commercial van traveling long distances between cities are provided based on the following conditions.

Working distance per year:	100,000 km
Diesel Lower Heating Value (D_{LHV}):	36 MJ/liter [19]
Maximum Thermal Efficient of 2.8-liter 1GD-FTV diesel engine ($Ther_{Eff}$):	44% [20]
Brake Horse Power (BHP):	154 Hp [20]
Wheel Horse Power (WHP):	140 Hp [20]
Average fuel consumption ($F_{avg, cons}$):	14.3 km/liter [21] (7 liter/100km)
Average speed (V):	90 km/h

The required driving powers, while an unmounted van travels at a constant speed of 90 km/h on a level road, consist of these five types of power:

1. Power to overcome air resistance.
2. Power to overcome the wheel's rolling friction.
3. Power loss by the drive train system.
4. Power loss by auxiliary electrical.
5. Power loss by parasitic.

The total 100% required driving power, P_{Total} (kW), is calculated from diesel energy consumption as the given condition.

$$P_{Total} = Diesel_{TEO}*V / F_{avg, cons} \qquad (3)$$

Relevant equations for calculating power loss.

Power to overcome air resistance, P_A (kW):

$$P_A = F_D V \qquad (4)$$

Power to overcome the wheel's rolling friction, P_{RF} (kW):

$$P_{RF} = F_r V \qquad (5)$$
$$F_r = C_R W \qquad (6)$$

Power loss percentage by drive system, P_{DT} (%):

$$BHP - WHP = HP_{Loss} \qquad (7)$$
$$P_{DT} = (HP_{Loss}/BHP)100 \qquad (8)$$

$Diesel_{TEO}$ is diesel thermal efficiency output, $D_{LHV}*Ther_{Eff}$ (MJ/liter), F_r is the rolling friction force, 0.0101 rolling coefficient (C_R), and W is the van's weight.

According to calculations based on equations (3), (8), and (11), it has been found that when a van travels at a constant speed of 90 km/h, the most significant portion of required driving power is caused by the power to overcome air resistance, accounting for 48.39% of the total required driving powers. Additionally, 34.04% of the power to overcome the wheel's rolling friction and 9.1% power to the drivetrain system for the other two required powers, The U.S. Department of Energy, Where the Energy Goes et al. (2008) [22] stated that there is power loss by parasitic (fuel and oil pump, engine control systems) is approximately 3 - 4% and power loss to auxiliary electrical is about 0 - 2% conducted as the vehicle cruising on the highway.

The percentage may not add up to 100% because there are differences in the vehicle tests conducted. However, this information can provide valuable insight into the critical areas of concern.

Almost half of a van's required driving power is due to air resistance; thus, addressing air resistance, aka drag force, is an effective solution to this critical issue.

Relevant equations for calculating saving and emission.
Power reduction due to lower drag coefficient, P_R (kW):

$$P_R = 11.6\%*P_A \qquad (9)$$

Energy/100km, E_n (kJ):

$$E_n = time*P_R \qquad (10)$$

Fuel Saving/100km, F_S (liter):

$$F_S = E_n / Diesel_{TEO} \qquad (11)$$

Cost saving (Bath/100km):

$$Cost\ saving = F_S*Diesel\ price \qquad (12)$$

Reduction rate of carbon dioxide emission (kg/100km):

$$CO_2 = Fuel_C*Diesel_{EF} \qquad (13)$$

$Fuel_C$ is fuel consumption (liter/100km), $Diesel_{EF}$ is the diesel emission factor (2.67 kg/liter) [23], and the Diesel price is 33.5 baht/liter.

This research found that the van with the rear roof spoiler potentially saved fuel up to 0.394 liters per hundred kilometers, saving 394 liters per year (100,000 km), or about 13,200 baht. The average fuel consumption changed from 14.3 to 15.15 kilometers per liter.

This change likely helped save fuel costs up to 5.63% annually. Comparing such fuel savings is equivalent to reducing carbon dioxide emissions by 1,052 kilograms per van per year.

5.0 CONCLUSION

This paper describes a computational study of the airflow around a van utilizing SolidWorks Flow Simulation. In particular, the impact of several attachment parts on the van's drag

coefficient is explored. The study found that a rear roof spoiler was the most effective aerodynamic part. By optimizing the spoiler's geometry, the optimal design for a rear roof spoiler was achieved.

Based on the flow simulation results, attaching the optimum rear roof spoiler could help reduce the van's drag coefficient by 11.6% (from 0.362 to 0.32). At a cruising speed of 90 kilometers per hour, fuel savings and CO_2 reduction are evaluated at 5.63%.

The results are significant to the automotive industry, as they offer insights into designing vehicles with improved aerodynamic performance. Reducing the drag coefficient is crucial for improving fuel efficiency and minimizing environmental impact.

Ultimately, this research proposes an energy conservation policy with low operating costs and substantial social value. It would reduce micro and macroeconomic energy use, lower overall fuel costs, and dramatically decrease carbon dioxide emissions.

Wind tunnel tests and road tests were planned for future studies to confirm the performance of the optimum rear roof spoiler.

Acknowledgment

Conflicts of Interest

The author(s) declare(s) that there is no conflict of interest regarding the publication of this paper

References

[1] Thai Government Gazette, *Ministerial Regulations No. 60 (B.E. 2552) issued under the Land Transport Act B.E. 2522.* 2552, 125 (31): 44 – 45. Ministry of Transport (Thailand), URL: https://rb.gy/9oi4r

[2] Department of Land Transport Planning Division Transport Statistics Group. 2022. Transport Statistics Report 2022. *Department of Land Transport (Thailand)*: 1 - 5. URL: https://web.dlt.go.th/statistics/

[3] Chowdhury, H., Moria, H., Ali, A., Khan, I., Alam, F., Watkins, S. 2013. A Study on Aerodynamic Drag of a Semi-trailer Truck. *Procedia Engineering, 56: 201-205, ISSN* 1877-7058. DOI: https://doi.org/10.1016/j.proeng.2013.03.108

[4] Huan, J., Modi, V. 1996. Design of minimum bodies in incompressible laminar flow. *Inverse Problems in Engineering*, 3(4): 233 - 260. DOI: https://doi.org/10.1080/174159796088027626

[5] Wang, J., Li, H., Liu, Y., Gao, H. 2018. Aerodynamic research of a racing car based on wind tunnel test and computational fluid dynamics. *MATEC Web Conf*. 153(04011): 5 DOI: https://doi.org/10.1051/matecconf/201815304011

[6] Gatto, A., Rejniak, A. A. 2022. Vehicle Having Reduced Drag. *United States Patent and Trademark Office*. US-20220410985-A1. URL: https://t.ly/eaook

[7] Moradnia, P, Metka, L. M, Rao, T. P. 2023. Wheel Casing. *United States Patent and Trademark Office*. US-20230013812-A1. URL: https://t.ly/eE8Rj\

[8] Rose, J. D., Metka, L. M., Rao, T. P., Torris, C. 2022. Active Spoiler. *United States Patent and Trademark Office*. US-20220402564-A1. URL: https://t.ly/d8Tvs

[9] Laipradit, W., Sorawat, M., Wansungnurn, P., Boonsuwan, K. 2000. Design of drag reduction device for pickup and bus. *Proceedings of the 38th Kasetsart University Annual Conference: Engineering, Agro-Industry. The 38th Academic Conference of Kasetsart University*. 61 - 65. URL: https://t.ly/klute

[10] Hariram, A., Koch, T., Mårdberg, B., Kyncl, J. 2019. A Study in Options to Improve Aerodynamic Profile of Heavy-Duty Vehicles in Europe. *Sustainability*. 11(19): 5519. DOI: https://doi.org/10.3390/su1119551 9

[11] Thai Government Gazette, *Ministerial Regulations Determine the speed rate for driving on the road B.E. 2564.* 2564, Prime Minister's Office (Thailand), 138 (77): 3. URL: https://rb.gy/dwm71

[12] Sobachkin, A., Dumnovl, G., Sobachkin, A. 2014. Numerical Basis of CAD-Embedded CFD. *NAFEMS World Congress, 2013,* J. 1999. Road Safety Through Video Detection. *Intelligent Transportation System.* 7 – 10. URL: https://rb.gy/sdwd4

[13] Çengel, A. Y., Cimbala, M. J. *Fluid Mechanics Fundamentals and Applications*. 2006. 1221 Avenue of the Americas, 9: 425 – 456. New York, NY, McGraw-Hill. URL: www.mhhe.com

[14] Toyota Motor Corporation, *Toyota HiAce Commuter Brochure,* 2022, 825 Third Ave., 10th Floor, New York, Toyota Tsusho America. URL: https://rb.gy/dabrp

[15] Anderson, J. D. *Fundamentals of aerodynamics / John D. Anderson, Jr. Sixth edition*. 2017. 2 Penn Plaza, New York, NY, McGraw-Hill Education, Chapter 5: 431. URL: http://lccn.loc.gov/2015040997

[16] Siddiqui, N. A., Asrar. W., Sulaeman, E. 2017. Literature Review: Biomimetic and Conventional Aircraft Wing Tips. *International Journal of Aviation, Aeronautics, and Aerospace, 4*(2): 6. DOI: https://doi.org/10.15394/ijaa.2017.1172

[17] Domel, A. G., Saadat, M., Weaver, J. C., Haj-Hariri, H., Bertoldi, K., Lauder, G. V. 2018. Shark skin-inspired designs that improve aerodynamic performance. *Journal of The Royal Society Interface.* 15: 20170828. DOI : http://dx.doi.org/10.1098/rsif.2017.0828

[18] Kim, J., Choi, H. 2014, Aerodynamics of golf ball with grooves. *Proceedings of the Institution of Mechanical Engineers, Part P: Journal of Sports Engineering and Technology*. 228(4): 233-241. DOI : https://doi.org/10.1177/1754337114543860

[19] Staffell, I. *The Energy and Fuel Data Sheet*. 2011. University of Birmingham, UK, The Claverton Energy Group. URL: https://rb.gy/63o6c

[20] Toyota Motor Corporation. 2015. *Toyota's Revamped Turbo Diesel Engines Offer More Torque, Greater Efficiency and Lower Emissions.* Global Toyota website, Jun 19 2015. URL: https://global.toyota/en/d etail/8348091/

[21] Saowamon, T. 2019, MG V80 VS TOYOTA COMMUTER. *4Wheels*, December (2019), Column: Test. URL: https://www.autoinfo.co.th/sp ecial/302572

[22] Oak Ridge National Laboratory. 2008. *Where the Energy Goes: Gasoline Vehicles*. The official U.S. government source for fuel economy information. Office of Energy Efficiency & Renewable Energy. U.S. Department of Energy. URL: https://www.fueleconomy.g ov/feg/atv.shtml

[23] Houghton, J. T., Filho Meira, L. G., Lim, B., Treanton, K., Mamaty, I., Bonduki, Y., Griggs, DJ., Callerder (Eds), BA. *Revised 1996 IPCC Guidelines for National Greenhouse Gas Inventories.* 1996. UK Meteorological Office, Bracknell, IPCC/OECD/IEA, Energy 2: 1.5 - 1.8 URL: https://rb.gy/l7upp